

Inelastic lateral-distortional buckling of continuously restrained continuous beams

Dong-Sik Lee†

4-6 Tangarra Street Croydon Park, NSW 2133, Australia

(Received February 16, 2004, Accepted April 13, 2005)

Abstract. The inelastic buckling behaviour of continuously restrained two and three-span continuous beams subjected to concentrated loads and uniformly distributed loads are studied in this paper. The restraint type considered in this paper is fully restrained against translation and elastic twist applied at the top flange. These types of restraints are most likely experienced in industrial structures, for example steel-concrete composite beams and half through girders. The buckling analysis of continuous beam consists of two parts, firstly the moment and shear distribution along the member are determined by employing force method and the information is then used for an out-of-plane buckling analysis. The finite element method is incorporated with so-called simplified and the polynomial pattern of residual stress. Owing to the inelastic response of the steel, both the in-plane and out-of-plane analysis, which is treated as being uncoupled, extend into the nonlinear range. This paper presents the results of inelastic lateral-torsional and lateral-distortional buckling load and finally conclusions are drawn regarding the web distortion.

Key words: buckling; continuous restraint; lateral-distortion; plasticity; finite elements; load-height; monosymmetry.

1. Introduction

The majority of research on buckling behaviour of steel structures have been limited to an unrestrained beam, which is restrained at the supports but unrestrained along the length of the member. Most industrial steel structures experience some sort of restraint, for example in continuous composite concrete-steel beams, and roof sheeting attached to industrial portal frames. These restraints are essentially continuous and furthermore the buckling load of the member may increase by the presence of these continuous restraints.

Limited research work has been conducted on both elastic and inelastic lateral-torsional buckling of restrained two and three-span continuous beams. Hancock and Trahair (1979) considered the elastic lateral-torsional buckling of continuously restrained two and three-span beams subjected to a uniformly distributed load using a line element with 8 buckling degrees of freedom. Bradford and Trahair (1986) studied the inelastic lateral-torsional buckling of restrained continuous beam-columns using a finite element method and verified it with an experimental study conducted by Cuk *et al.* (1986). The main assumption of lateral-torsional buckling is that the flange displaces and twists as a rigid body without web distortion, but this assumption is questionable when the beam is restrained, where the cross-section

†E-mail: leehansol@hotmail.com

necessarily experiences web distortion if it is buckle out-of-plane. Essa and Kennedy (1994) examined a collapsed roof structure in Canada. The roof structure was a concrete-steel composite section where the metal deck, which acted compositely with the concrete slab, was supported by cantilever-suspended span steel I-beams and open web steel trusses. The metal deck acted as restraint to prevent lateral displacement and twist of the beam. The region of the roof structure that collapsed was subjected to negative bending. Essa and Kennedy (1994) analysed the collapsed roof structure incorporating residual stress and lateral and torsional restraint, and they also included the effects of the load height. Essa and Kennedy (1994) have shown that the reductions of the lateral-torsional buckling load due to web distortion for restrained I-section members are significant, and furthermore neglecting the effect of web distortion of beam subjected to a continuous restraint may cause a premature ultimate failure of the structure. However, the inelastic lateral-distortional buckling of I-sections has not received as much attention due to the complexity of the analysis.

Lee and Bradford (2002, 2003) studied the inelastic lateral-distortional buckling of continuously restrained simply supported beams subjected to a uniform bending and a cantilevered beam respectively. Johnson and Bradford (1983) and Bradford and Johnson (1987) considered composite cross-sections, while Bradford and Gao (1992) considered the elastic lateral-distortional buckling of continuous composite beams. Dekker *et al.* (1995) considered the factors influencing the strength of composite beams in negative bending and a theoretical model was developed by introducing an equivalent spring system to account for the effect of the web distortion. A finding of Dekker *et al.* (1995) was that the flexural resistance of the steel beam is controlled by lateral-distortional buckling for the case of inelastic buckling. Kemp *et al.* (1995) considered the inelastic buckling behaviour of continuous steel and composite beams by considering two-span continuous beams subjected to uniformly distributed loads.

This study considers inelastic lateral-torsional and lateral-distortional buckling of two and three-span beams under a transverse load applied at the top flange, which is fully restrained against translation and elastic twist restraint applied at the top flange. The line-element deployed in this study is a 16-degree of freedom per element. Kitipornchai and Trahair (1975) found from their experimental study that the maximum compressive residual stress at the flange tip is relatively small but the maximum tensile residual stresses in the flange-web junction are high for slender I-section beam, while the compact I-section has shown that the maximum compressive residual stress at the flange is higher than the maximum tensile residual stresses in the flange-web junction. Therefore the residual stresses adopted in this study are the polynomial and the well-known simplified pattern. The distribution of polynomial residual stress is quartic in the flange and parabolic distribution in the web, which satisfies the compact and slender I-sections. The numerical study of inelastic lateral-torsional and inelastic lateral-distortional buckling of continuous beam is undertaken by considering two I-sections to illustrate the lateral-distortion buckling behaviour of the I-sections. Furthermore, these inelastic buckling results are compared with the 'design by buckling analysis' of AS4100 (1998).

2. Finite element method

2.1. General

Fig. 1(a) shows a beam element with reference axis system located at mid height of the web. Figs. 1(b) and 1(c) show the applied moment M_1 , M_2 and shear force V_1 , V_2 of the element. The beam element is

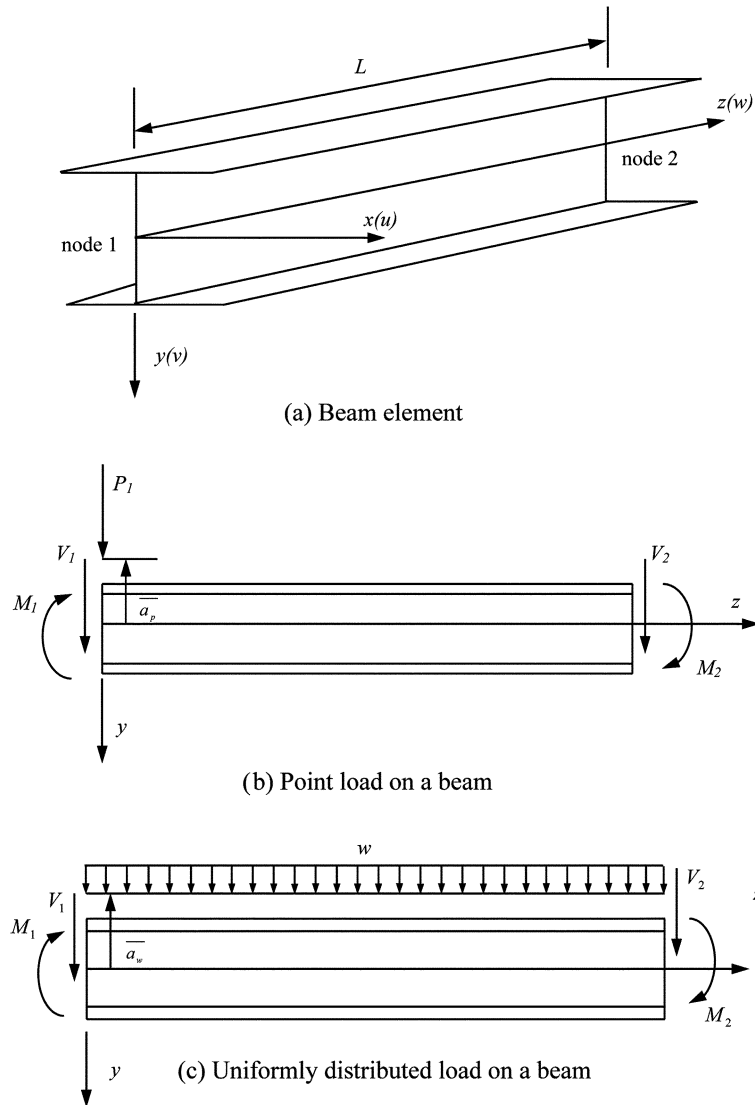


Fig. 1 Beam element and loading

also subjected to a concentrated load P_1 at node 1 positioned \bar{a}_p and a uniformly distributed load w positioned \bar{a}_w above the reference axis. The buckling analysis of restrained continuous beams consists of two phases: firstly, an in-plane bending analysis to establish the applied curvature and elastic and yielded, and strain-hardened region of the cross-section. The determination of the applied bending moment along the beam is not easy because of indeterminacy due to continuity of beam. An in-plane bending analysis is performed using the well-known force method (Hall and Kabaila 1986) to determine the reaction at the internal supports, and simple statics is then used to determine the moment and shear force along the beam. The second phase of analysis is an out-of-plane buckling using the line-element. The line element adopted in this study is 16 degrees of freedom. A detailed method of the out-of-plane buckling analysis is given in Lee and Bradford (2003) and Lee (2004). Figs. 2(a) and 2(b)

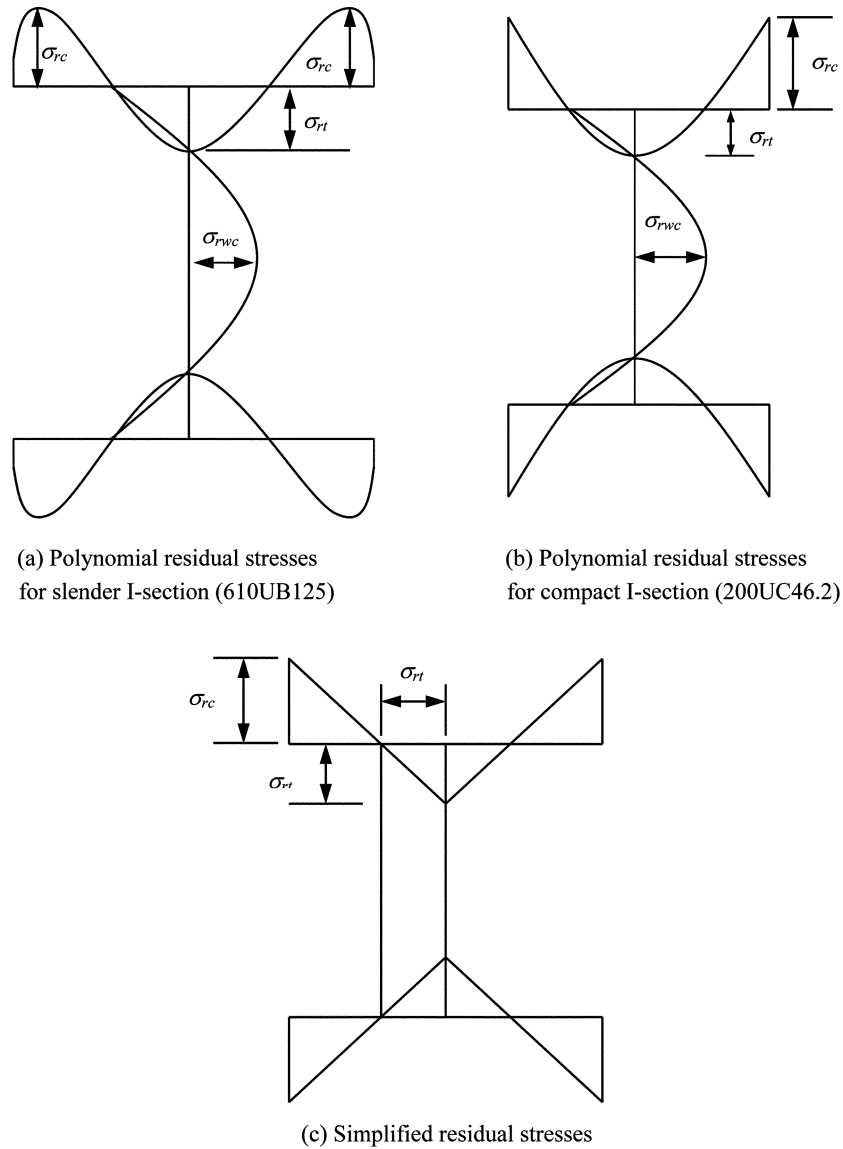


Fig. 2 Residual stress models

show the polynomial pattern of residual stress for slender I-section and for compact I-section respectively, while the simplified pattern of residual is shown in Fig. 2(c). The distribution of residual stress in the flange and the web with maximum residual stresses in the flange and the flange-web junction is given in Lee (2004).

2.2. In-plane analysis

This study considers the two and three-span continuous beams subjected to a central concentrated load at mid span of all spans and a uniformly distributed load. The method adopted in this study to

determine the internal reactions is well-known force method (Hall and Kabaila 1986). The determination of the internal support reactions is given as:

For a two-span continuous beams

$$u_1 = \int \frac{M_0 m_1}{EI_x} dx + x_1 \int \frac{m_1^2}{EI_x} dx \tag{1}$$

For a three span continuous beams

$$\begin{bmatrix} \int \frac{M_0 m_1}{EI_x} dx \\ \int \frac{M_0 m_2}{EI_x} dx \end{bmatrix} + \begin{bmatrix} \int \frac{m_1^2}{EI_x} dx & \int \frac{m_1 m_2}{EI_x} dx \\ \int \frac{m_2 m_1}{EI_x} dx & \int \frac{m_2^2}{EI_x} dx \end{bmatrix} \begin{bmatrix} x_1 \\ x_2 \end{bmatrix} = \begin{bmatrix} u_1 \\ u_2 \end{bmatrix} \tag{2}$$

where the internal displacements are denoted as u_1, u_2 at the supports, and x_1, x_2 are redundant actions.

The determination of internal reaction for a two-span continuous beams subjected to a central concentrated load is shown in Fig. 3(a). The moment due to the applied load on the primary structure and the moments due to unit values of the redundant actions is represented as M_o and m_1 respectively as shows in Figs. 3(b) and 3(c). The integral Eqs. (1) and (2) are to determine by two-point Gaussian quadrature. The distribution of the moment and shear force along the beam can be determined from simple statics.

For a two-span continuous beams subjected to a central concentrated load:

$$M_x = R_1 z - P \left\langle z - \frac{L_1}{2} \right\rangle + R_2 \langle z - L_1 \rangle - P \left\langle z - L_1 - \frac{L_2}{2} \right\rangle \tag{3}$$

and for a three-span continuous beams subjected to a concentrated load:

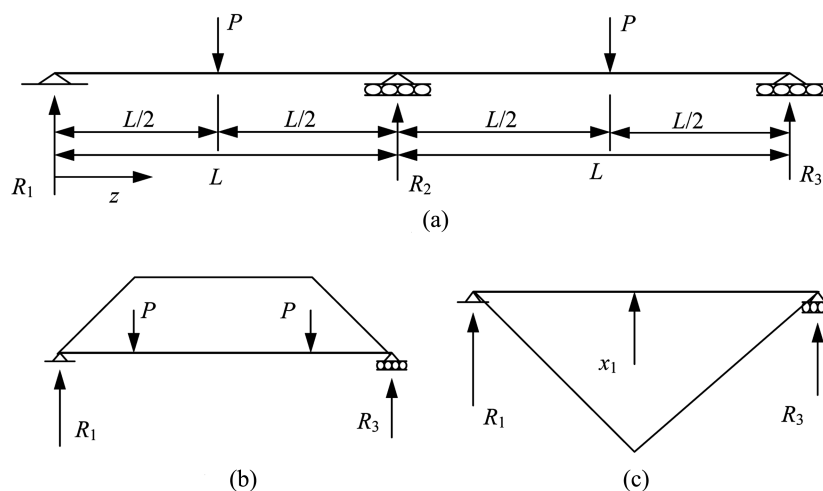


Fig. 3 (a) Two-span continuous beam subjected to a concentrated load, (b) moment diagram for M_o , (c) moment diagram for m_1

$$M_x = R_1 z - P \left\langle z - \frac{L_1}{2} \right\rangle + R_2 \langle z - L_1 \rangle - P \left\langle z - L_1 - \frac{L_2}{2} \right\rangle + R_3 \langle z - L_1 - L_2 \rangle - P \left\langle z - L_1 - L_2 - \frac{L_3}{2} \right\rangle \quad (4)$$

while for a two-span continuous beams subjected to a uniformly distributed load:

$$M_x = R_1 z - \frac{wz^2}{2} + R_2 \langle z - L_1 \rangle \quad (5)$$

and for a three-span continuous beams subjected to a uniformly distributed load:

$$M_x = R_1 z - \frac{wz^2}{2} + R_2 \langle z - L_1 \rangle + R_3 \langle z - L_1 - L_2 \rangle \quad (6)$$

where the Macaulay bracket $\langle \rangle$ term is taken as zero when the quantity inside the Macaulay bracket is not positive.

The determination of the major axis flexural rigidity EI_x in inelastic buckling analysis of continuous beams is more complicated than those of elastic analysis. The flexural rigidities EI_x along the beam are depended on the applied load and are not constant along the member due to the variation of the degree of yielding along the beam. The flexural rigidities about the major axis is determined using secant modulus theory as

$$\rho = \frac{M_x}{EI_x} \quad (7)$$

where ρ is applied curvature.

Due to the initially unknown quantity of flexural rigidity EI_x , an iterative method is employed to perform an in-plane analysis. A trilinear idealisation of the stress-strain curve is assumed in this study as shows in Fig. 4. This study assumes that the shear does not influence the yielding of the member. The curvature and the distribution of the elastic and inelastic regions of the cross-section are determined iteratively. Firstly, discretised the beam into number of elements and assumed the value of applied load, and flexural rigidity EI_x (elastic value of flexural rigidity is taken initially) at each node. The internal support reactions can be calculated using the force method (Eq. 1 for two-span continuous beams and

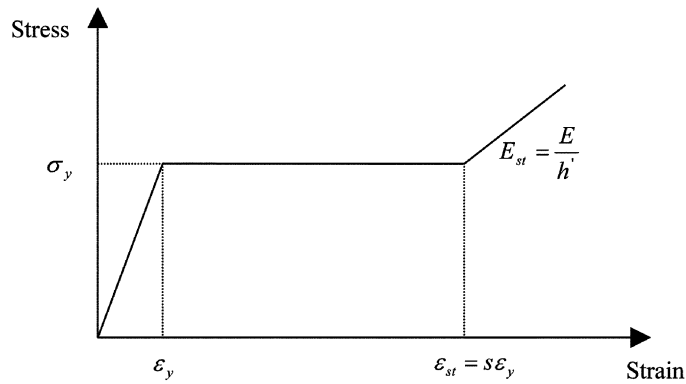


Fig. 4 Trilinear stress-strain idealization

Eq. 2 for three-span continuous beams) and the distribution of the moment and shear force along the beam can be determined using simple statics as shows in Eqs. (3) to (6). The elastic and inelastic regions of the cross-section and curvature can be determined using the non-linear moment-curvature relationship (Lee and Bradford 2002, 2003) with the predetermined moment along the beam. The flexural rigidity EI_x can then be calculated again using Eq. (7) with the known value of curvature and moment distribution along the beam. If the difference between the assumed value of EI_x and calculated value of EI_x is more than 0.002% of the elastic major axis of flexural rigidity, a new value of EI_x is chosen and the process repeated until a tolerance within 0.002% of the elastic major axis of flexural rigidity is obtained.

2.3. Out-of-plane analysis

An out-of-plane buckling deformation of the cross-section shows in Fig. 5 and the buckling deformation and twist of the flange expresses as u and ϕ respectively. The subscript T and B are represented as the top and the bottom flange respectively. The displacement of the flange $\{u\} = \langle u_T, u_B, \phi_T, \phi_B \rangle$ for element assumes to be cubic polynomial in z direction, and the buckling deformation of the element $\{\delta\}$ can be expressed as $\{u_{T1}, u'_{T1}, u_{B1}, u'_{B1}, \phi_{T1}, \phi'_{T1}, \phi_{B1}, \phi'_{B1}, u_{T2}, u'_{T2}, u_{B2}, u'_{B2}, \phi_{T2}, \phi'_{T2}, \phi_{B2}, \phi'_{B2}\}$. The web buckling deformation u_w assumes the cubic curve in y direction. The buckling displacement of the web can be expressed in terms of buckling deformation of the element using the compatibility condition between flange-web junctions.

The strain energy stored in the beam element can be written as

$$U = U_F + U_W + U_R \tag{8}$$

where U_F and U_W is the strain energy due to the flange and the web respectively, and U_R is the strain energy due the continuous elastic restraint.

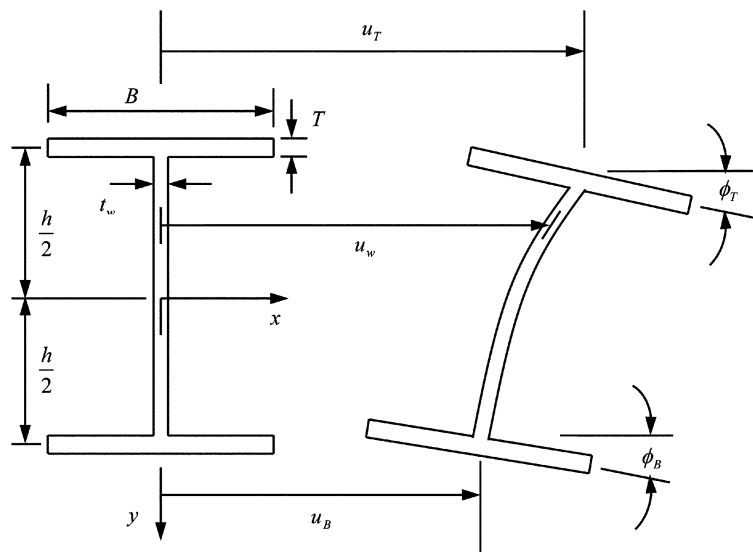


Fig. 5 Buckling deformations of a cross-section

The stiffness matrices of flange $[k_F]$ can be determined as was done by Trahair and Kitipornchai (1972), and Lee and Bradford (2002, 2003) by employing tangent modulus theory. A detail description of the method to determine the minor axis flexural and the torsional rigidities is given in those papers. The stiffness matrices of web $[k_W]$ can be determined using isotropic plate theory (Timoshenko and Woinowsky-Krieger 1959) for the elastic region and orthotropic plate theory based on flow theory (Dawe and Kulak 1984, Haaijer 1957) is used for the inelastic region. The patterns of residual stresses considered in this study are the polynomial and the simplified pattern. The simplified pattern of residual stresses was used by number of researchers (Fukumoto and Galambos 1966, Trahair and Kitipornchai 1972, Abdel-Sayed and Aglan 1973) to study the inelastic buckling behaviour of the I-section beam. The simplified pattern of residual stresses satisfies the static equilibrium condition but not that with axial torque and

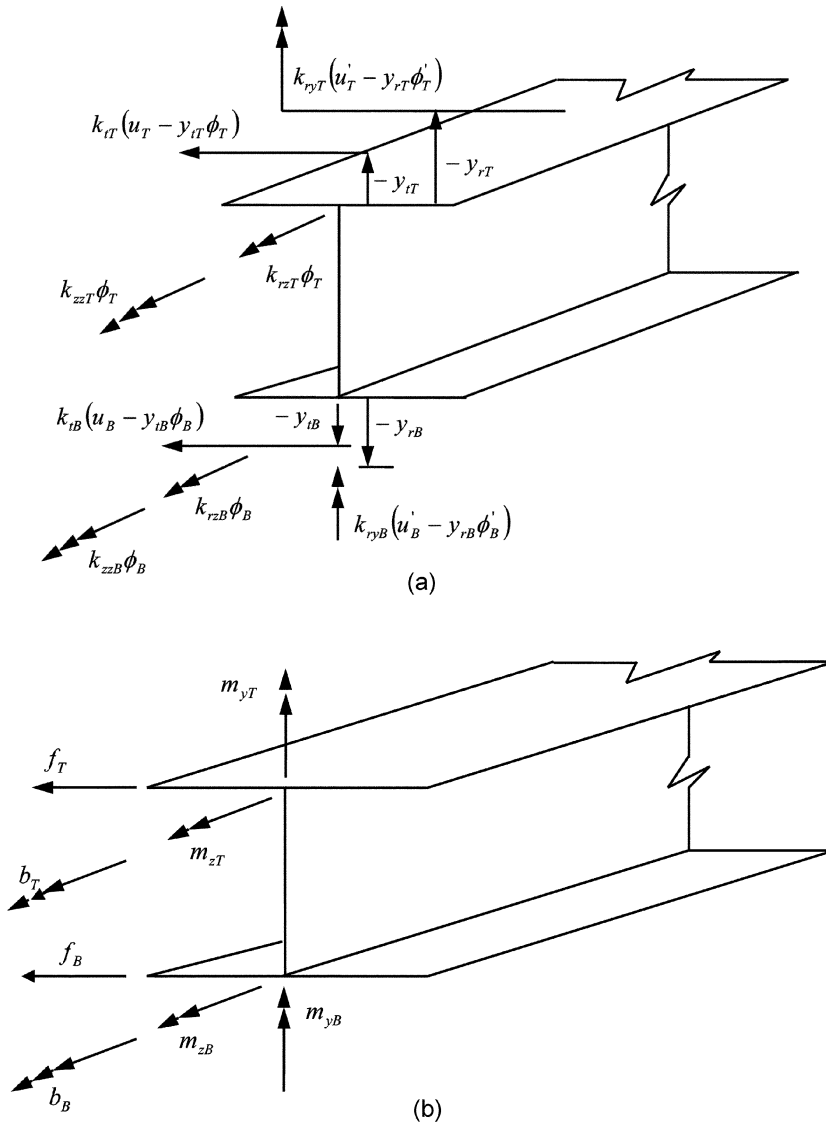


Fig. 6 (a) Elastic restraints, (b) Restraining actions applied at the flanges

therefore the torsional rigidity of the cross section alters to $\left((GJ)_t - \int_A \sigma_r(x^2 + y^2) dA \right)$ as was noted by Trahair (1993).

The continuous elastic restraint is augmented in this study as was done by Lee and Bradford (2002, 2003). Figs. 6(a) and (b) show the continuous restraints which act on a beam. The translation restraint applied at the top and the bottom flange is denoted as k_{tT} and k_{tB} respectively. The minor axis rotational restraints on the top and the bottom flange represents as k_{ryT} and k_{ryB} respectively. These restraints act at distance y_t and y_B above the top flange and below the bottom flange respectively. The torsional and warping restraints represent as k_{rz} and k_{zz} respectively.

The strain energy stored in the beam element can be expressed in stiffness matrix of the element

$$[k] = [k_F] + [k_W] + [k_R] \quad (9)$$

It must be note that the stiffness matrices of the flange $[k_F]$ and the web $[k_W]$ are not constant due to monosymmetric effect caused by combination of the applied curvature and the residual stresses.

The loss of total potential energy due to the applied bending moment and shear force and height of application of the load can be written as

$$W = W_F + W_W + W_{\bar{a}} \quad (10)$$

where W_F and W_W is the work done by the flange and the web respectively, and $W_{\bar{a}}$ is the work done by height of the load above the reference axis.

The loss of total potential energy in element can be expressed in terms of stability matrix of the element as:

$$[g] = [g_F] + [g_W] + [g_{\bar{a}}] \quad (11)$$

where $[g_F]$ and $[g_W]$ is the stability matrices of the flange and the web respectively, and $[g_{\bar{a}}]$ is the stability matrix due to the height of load above the reference axis.

2.4. Buckling solution

The element stiffness matrix $[k]$ and stability matrix $[g]$ can be assembled into global stiffness matrix $[K]$ and stability matrix $[G]$ and is give as;

$$([K] - \lambda[G])\{q\} = 0 \quad (12)$$

where $\{q\}$ is the buckling deformation (eigenvector). The stiffness and stability matrix is function of the applied curvature and the global stiffness and stability matrix is therefore adjusted at a value of applied curvature. Thus an iterative method is employed to determine the buckling solution until the determinant of equation 12 vanishes.

3. Inelastic lateral-distortional buckling of restrained continuous beams

This study considers two and three-span continuous beams subjected to a concentrated load at the mid point of all spans and a uniformly distributed load applied at the top flange, which is fully restrained against translation with an elastic twist restraint applied at the top flange. The number of

element used in this study is 8 per span. The material properties are E (Elastic modulus) = 200 GPa, ν (Poisson's ratio) = 0.3, $h'(E/E_{st}) = 33$ and $s(\varepsilon_{st}/\varepsilon_y) = 11$, and σ_y (yield stress) = 250 MPa. The cross-sections used in this study are 200UC46.2 (which has similar dimensions to the widely researched 8WF31) and 610UB125 (BHP 1988). The results are plotted in figures with the dimensionless buckling load (M_I/M_P), as a function of the dimensionless length $\sqrt{M_P/M_{EL}}$. M_I is inelastic buckling moment and M_P is plastic moment, and M_{EL} is the elastic lateral-torsional buckling moment which can be obtained high value of yield stress without residual stress. The figures also show buckling curves derived from the 'design by buckling analysis' of AS4100 (1998). The inelastic lateral-torsional buckling results are also shown in the figures. The elastic and inelastic lateral-torsional buckling results can be obtained by suppressing an out-of-plane web distortion as was done by Bradford and Trahair (1982).

$$U_{wP} = \frac{1}{2} \gamma_r \int_0^{\frac{h}{2}} \int_0^{\frac{L}{2}} D_w \left(\frac{\partial^2 u_w}{\partial y^2} \right) dy dz \quad (13)$$

where $D_w = E t_w^3 / 12(1-\nu^2)$ and γ_r is set to a large value (say 10^8).

A dimensionless torsional parameter α_z is used in this study and is given as;

$$\alpha_z = \frac{k_z L^2}{\pi^2 GJ} \quad (14)$$

where GJ is the torsional rigidity, L is length of the beam and k_z is the torsional restraint.

3.1. Two-span continuous beams

This study considers equal length and unequal length continuous beams subjected to a central concentrated load and a uniformly distributed load that is applied at the top flange. The inelastic buckling results for an equal span continuous beams subjected to a central concentrated load on both spans with the dimensionless torsional parameter α_z equal to 0, 1, 100 and 1000 are shown in Figs. 7 to 10, while Figs. 11 and 12 are for unequal span subjected to a central concentrated load in both span at a value of α_z equal to 100 and 1000. The buckling results for the equal span continuous beams under a uniformly distributed load at a value of α_z equal to 0, 1, and 100 are shown in Figs. 13, 14 and 15, while Figs. 16 and 17 are for unequal span at a value of α_z equal to 100 and 1000. As would be expected, the buckling mode of two-span beams is lateral-torsional when the beam is subjected to a translational restraint only ($\alpha_z = 0$). Generally speaking, as the dimensionless torsional parameter α_z increases from 0 to 1000 the buckling mode becomes lateral-distortional rather than a lateral-torsional. The severity of web distortion is greatest when $\alpha_z = 1000$. The result for the 200UC46.2 cross-section show that the reduction of lateral-torsional buckling loads due to web distortion is insignificant.

It can be seen in the figures that the 'design by buckling analysis' in AS4100 (1998) is generally unconservative for both slender and compact I-sections. The beam becomes more unconservative as the dimensionless length $\sqrt{M_P/M_{EL}}$ is decreased for slender (610UB125) beam at a lower value of torsional stiffness ($\alpha_z = 0$ and 1). When the torsional stiffness α_z is 100 and 1000, the disparity between 'design by buckling analysis' in AS4100 (1998) and inelastic buckling load is increased. The inelastic buckling moment of compact I-section (200UC46.2) reaches its plastic moment at lower value torsional stiffness ($\alpha_z = 0$ and 1).

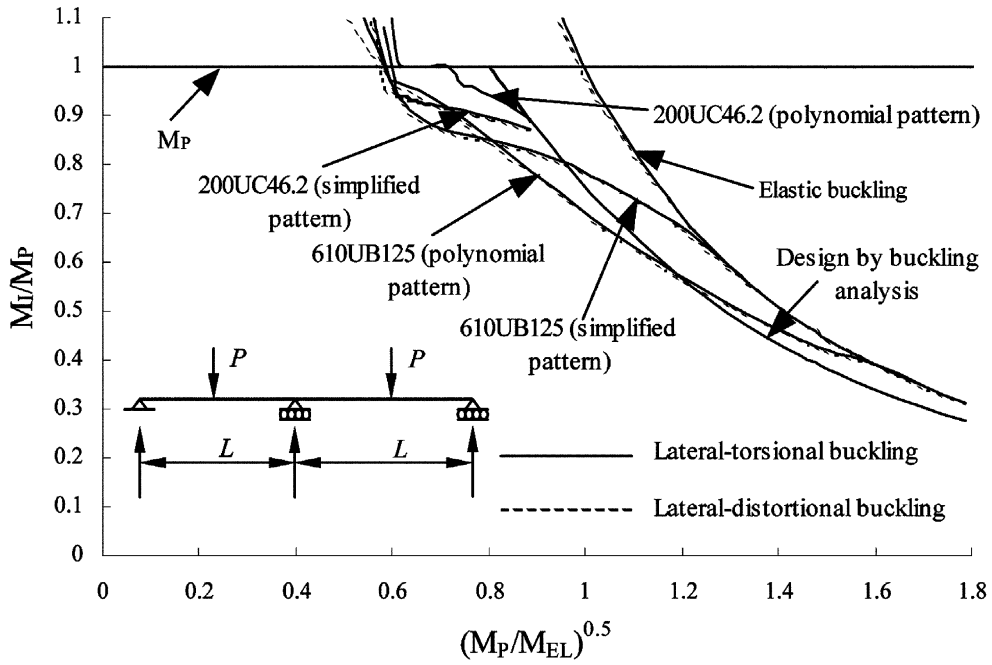


Fig. 7 Inelastic buckling of two-span continuous beam with elastic twist restraint ($\alpha_z = 0$)

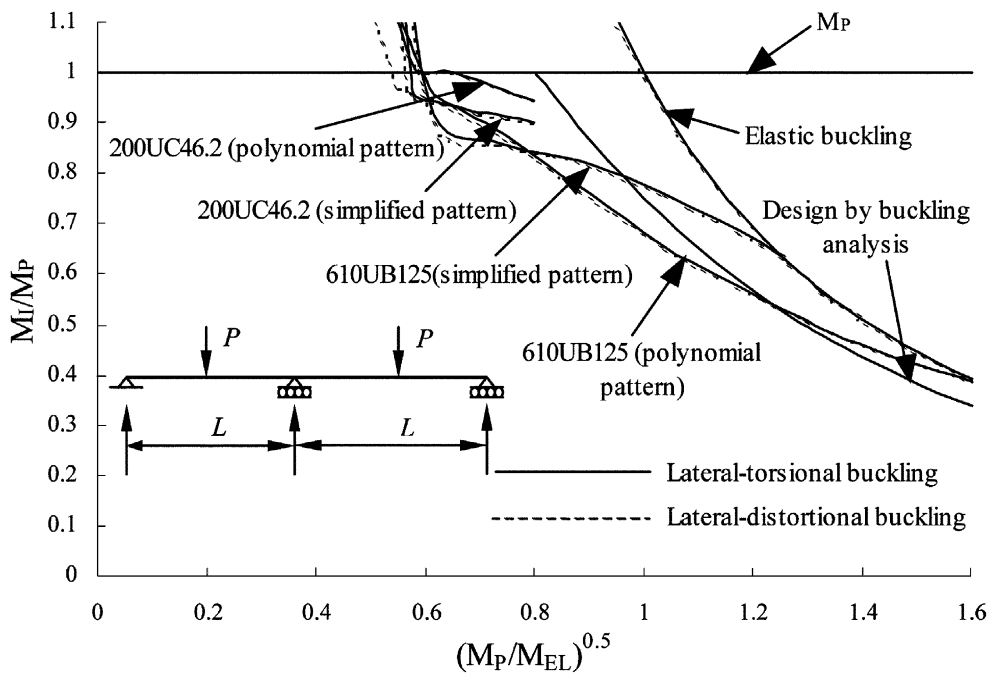


Fig. 8 Inelastic buckling of two-span continuous beam with elastic twist restraint ($\alpha_z = 1$)

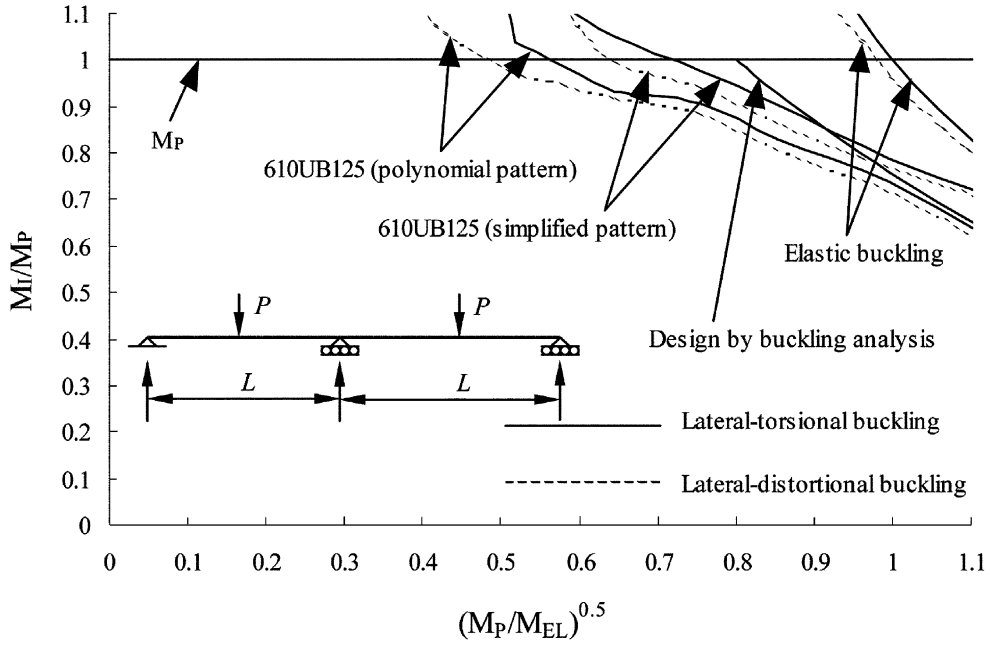


Fig. 9 Inelastic buckling of two-span continuous beam with elastic twist restraint ($\alpha_z = 100$)

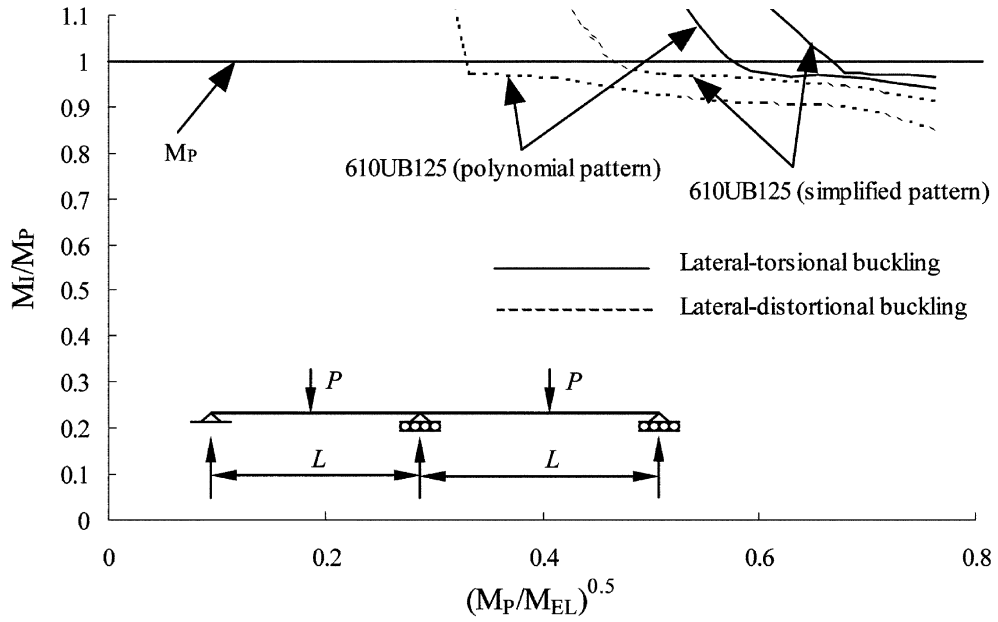


Fig. 10 Inelastic buckling of two-span continuous beam with elastic twist restraint ($\alpha_z = 1000$)

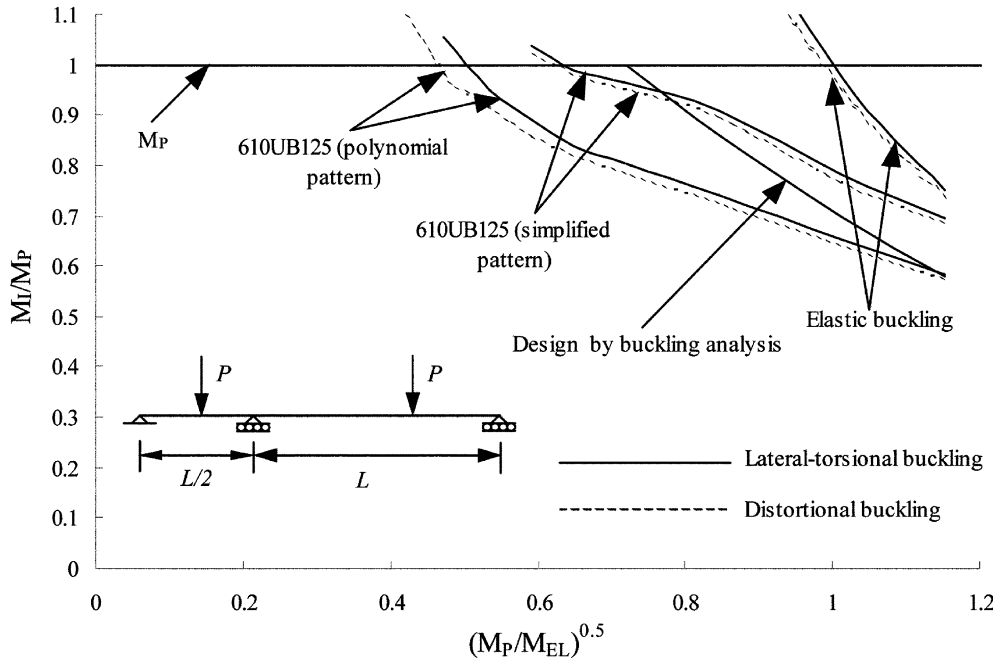


Fig. 11 Inelastic buckling of two-span continuous beam with elastic twist restraint ($\alpha_z = 100$)

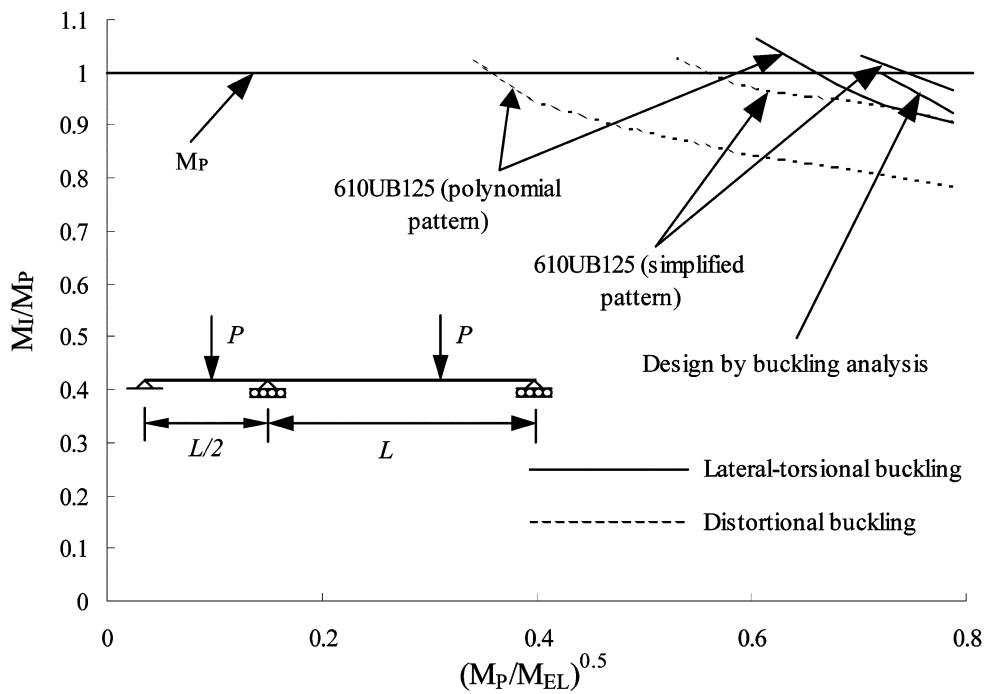


Fig. 12 Inelastic buckling of two-span continuous beam with elastic twist restraint ($\alpha_z = 1000$)

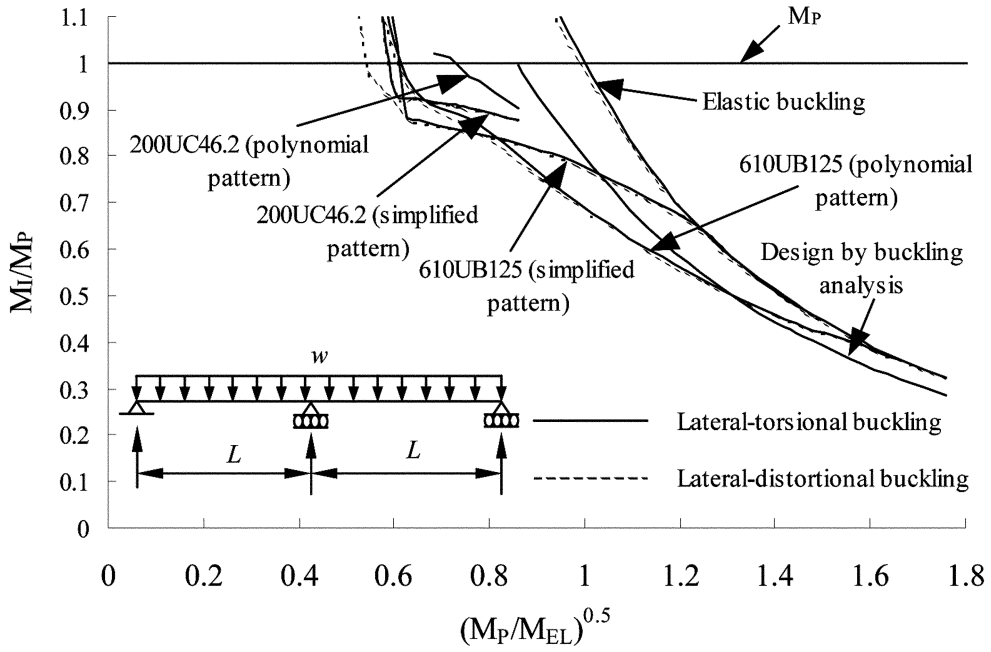


Fig. 13 Inelastic buckling of two-span continuous beam with elastic twist restraint ($\alpha_c = 0$)

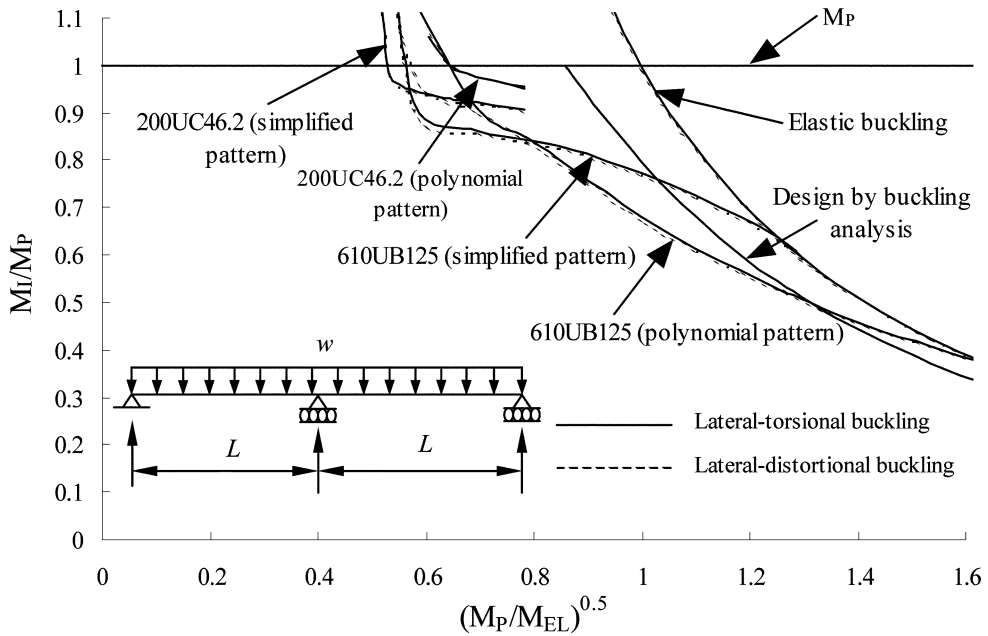


Fig. 14 Inelastic buckling of two-span continuous beam with elastic twist restraint ($\alpha_c = 1$)

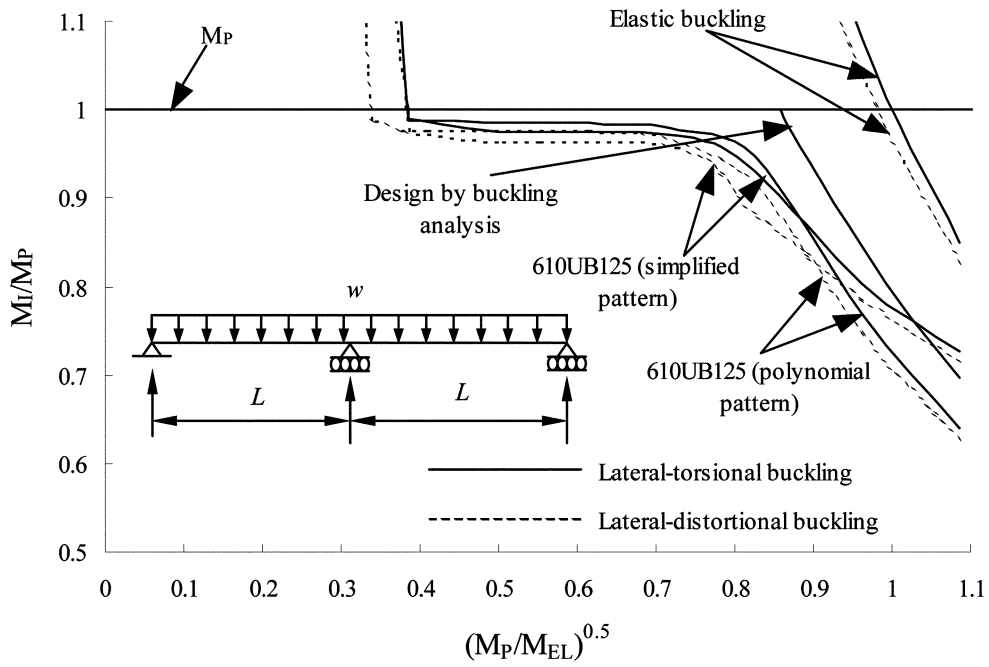


Fig. 15 Inelastic buckling of two-span continuous beam with elastic twist restraint ($\alpha_z = 100$)

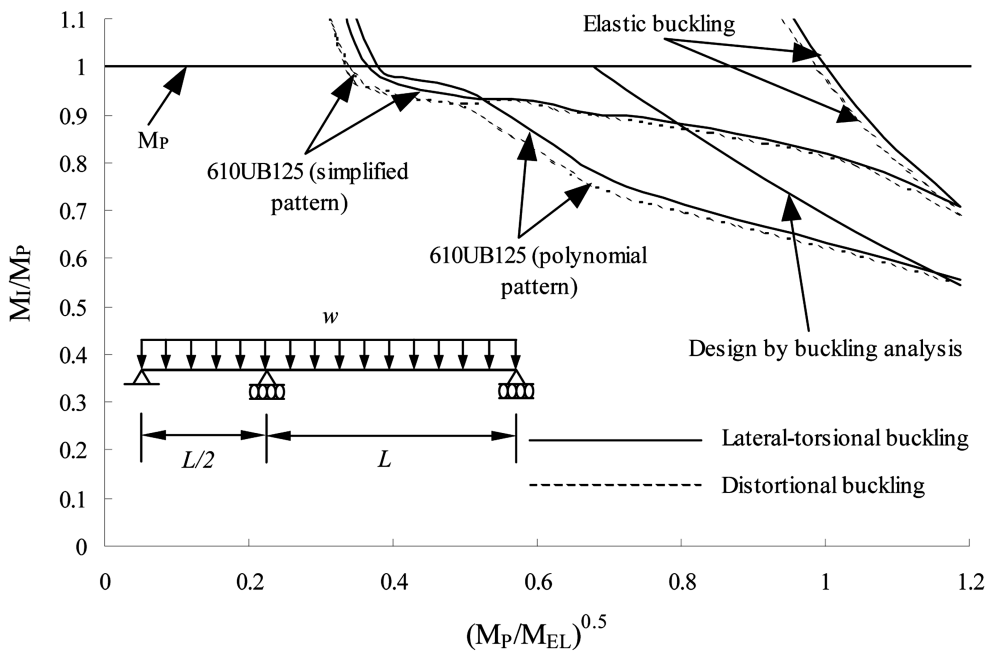


Fig. 16 Inelastic buckling of two-span continuous beam with elastic twist restraint ($\alpha_z = 100$)

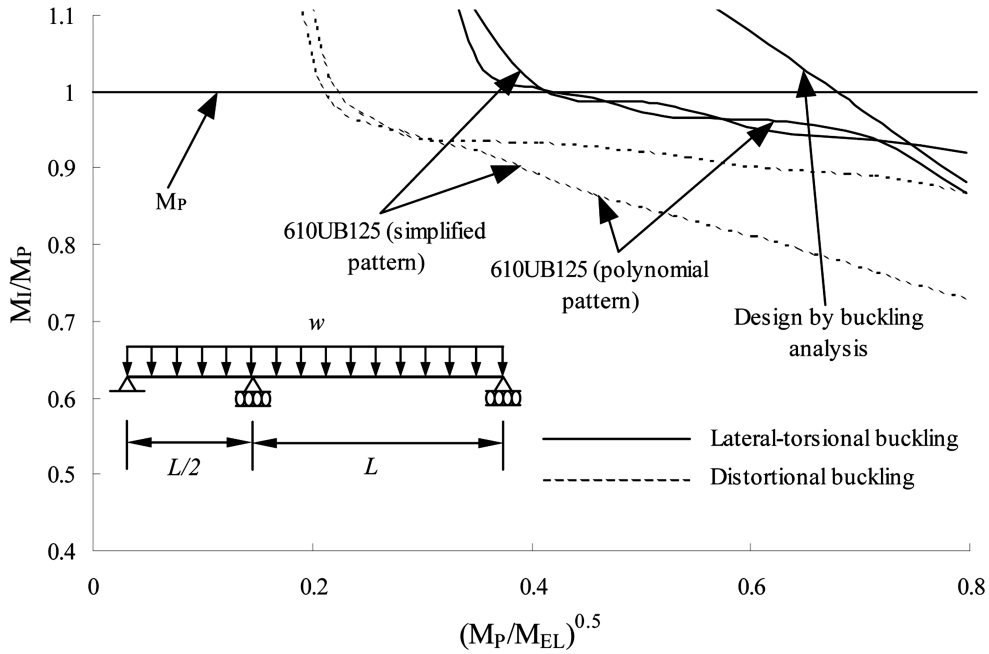


Fig. 17 Inelastic buckling of two-span continuous beam with elastic twist restraint ($\alpha_z = 1000$)

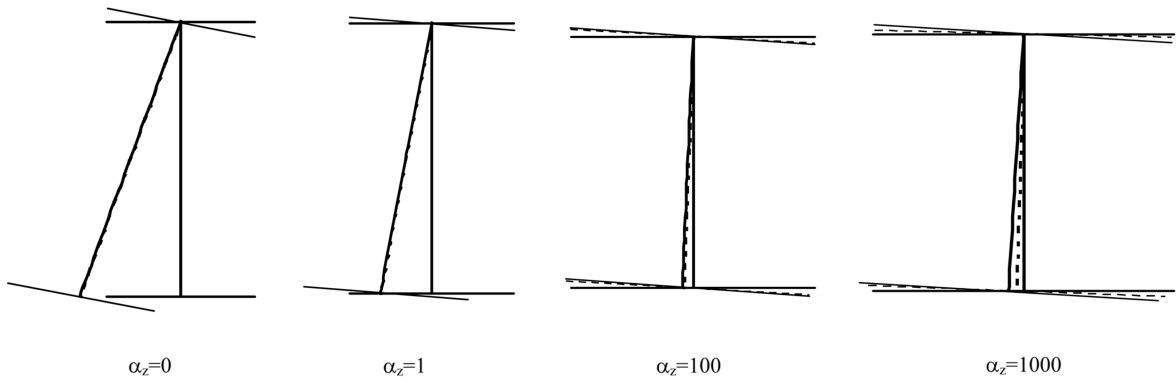


Fig. 18 Buckling mode of restrained two span continuous beam

Fig. 18 shows the buckling shape $\{q\}$ obtained from the eigensolver for an equal length two-span 610UB125 continuous beams subjected to a concentrated load at the mid point of both spans with $L/h = 160$. The dash and dotted lines indicate lateral-torsional and lateral-distortional buckling respectively. It can be seen in the Fig. 18 that the lateral-torsional buckling behaviour of two-span continuous beams is not affected by web distortion when the top flange is fully restrained against translation only ($\alpha_z = 0$). As α_z is increased the buckling mode of the two-span beams becomes a lateral-distortional one rather than a lateral-torsional one.

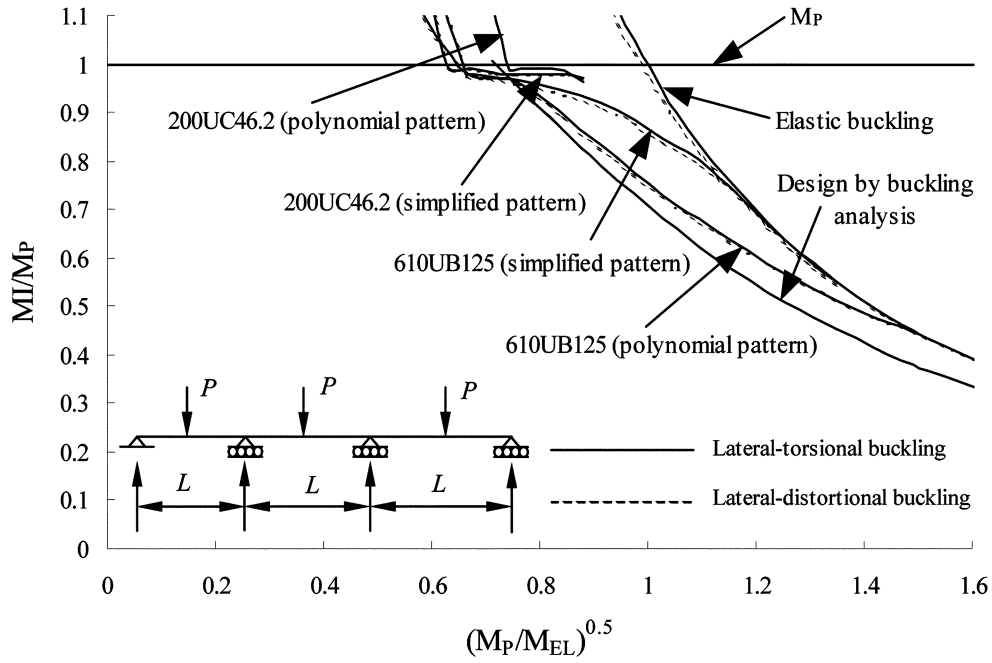


Fig. 19 Inelastic buckling of three-span continuous beam with elastic twist restraint ($\alpha_z = 0$)

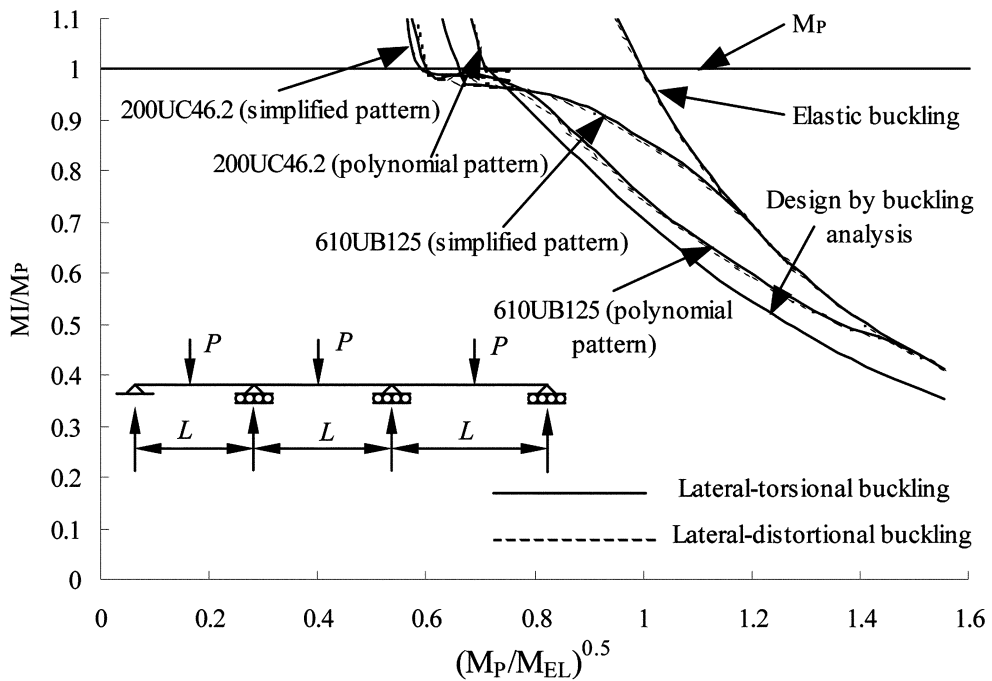


Fig. 20 Inelastic buckling of three-span continuous beam with elastic twist restraint ($\alpha_z = 1$)

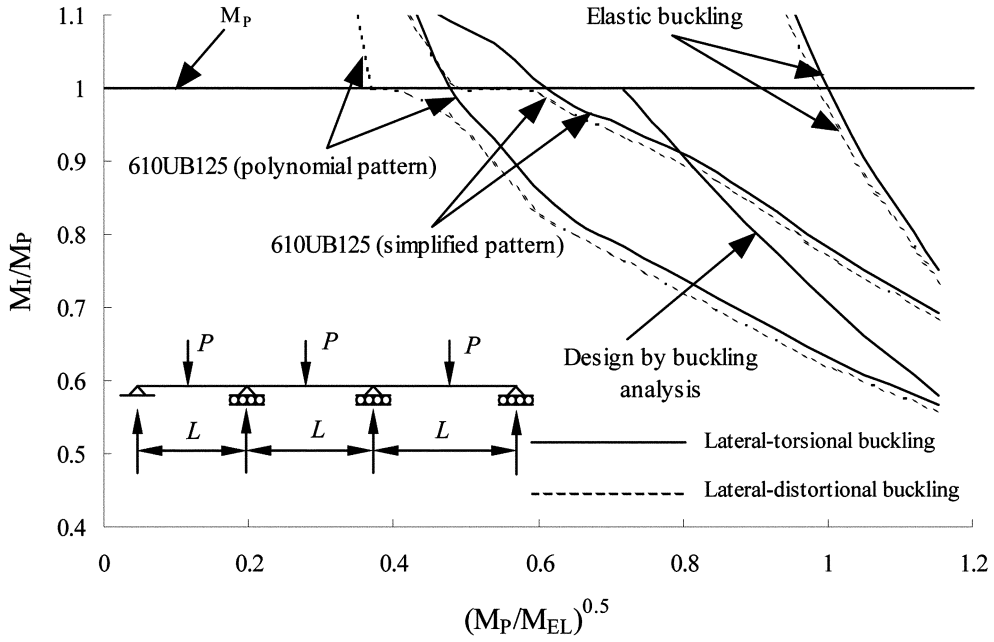


Fig. 21 Inelastic buckling of three-span continuous beam with elastic twist restraint ($\alpha_z = 100$)

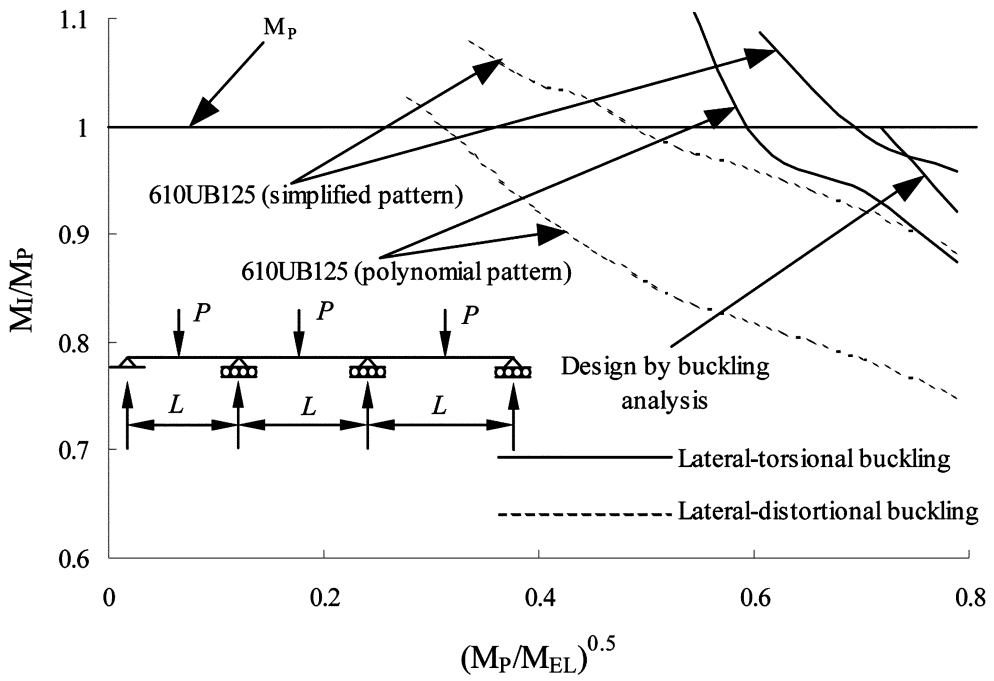


Fig. 22 Inelastic buckling of three-span continuous beam with elastic twist restraint ($\alpha_z = 1000$)

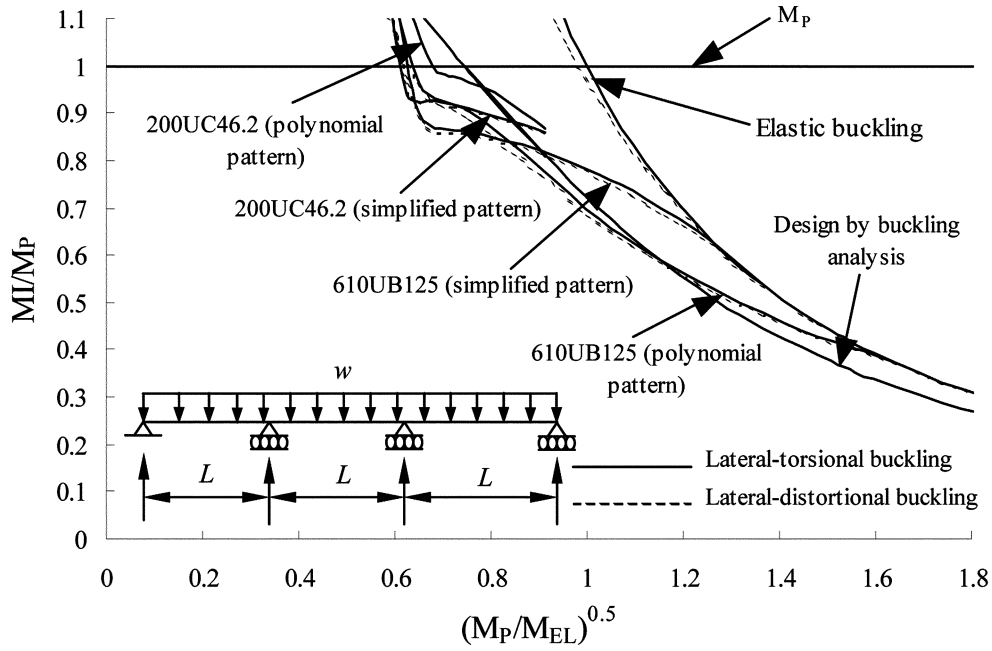


Fig. 23 Inelastic buckling of two-span continuous beam with elastic twist restraint ($\alpha_z = 0$)

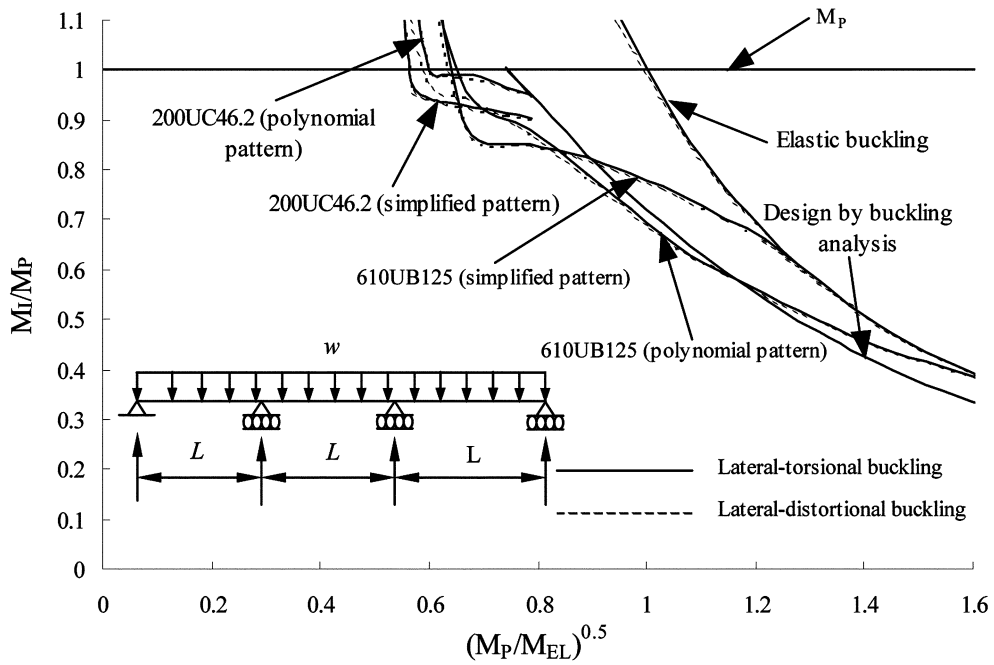


Fig. 24 Inelastic buckling of three-span continuous beam with elastic twist restraint ($\alpha_z = 1$)

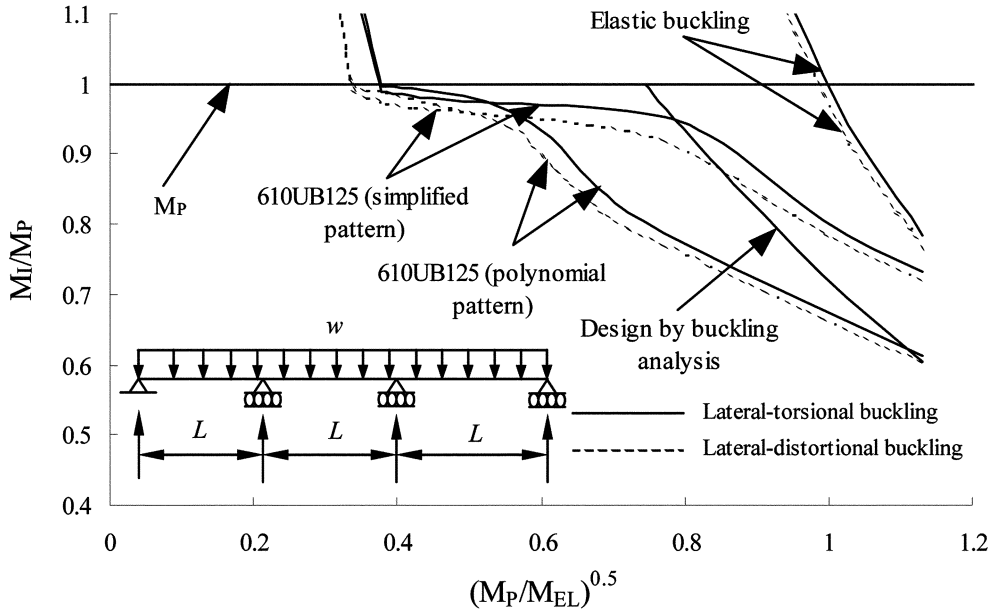


Fig. 25 Inelastic buckling of three-span continuous beam with elastic twist restraint ($\alpha_z = 100$)

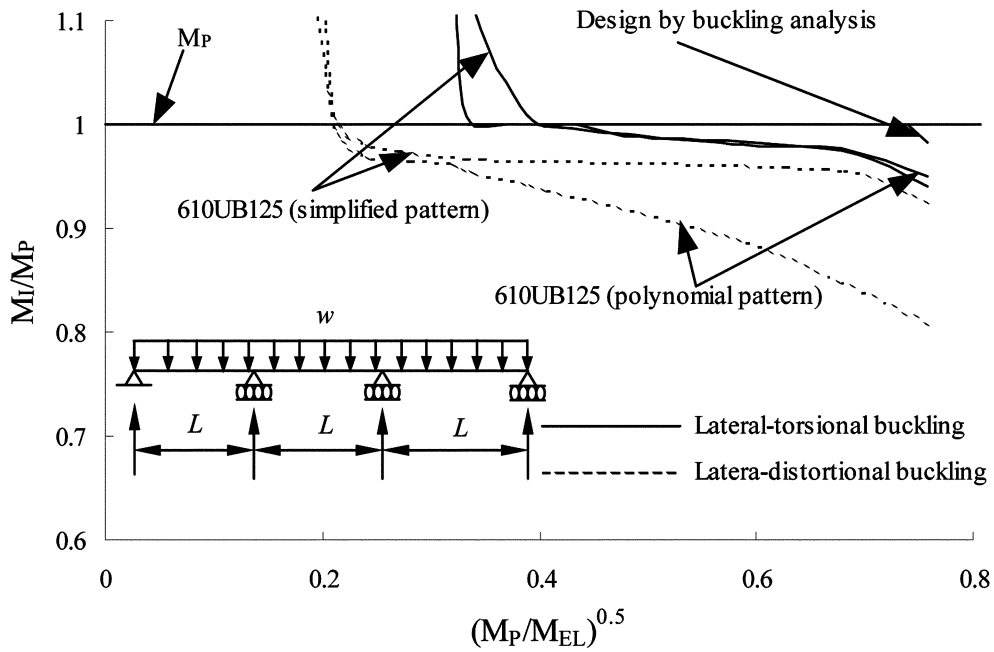


Fig. 26 Inelastic buckling of three-span continuous beam with elastic twist restraint ($\alpha_z = 1000$)

3.2. Three-span continuous beams

The buckling results for three-span continuous beams subjected to a concentrated load at the mid point of each spans at a value of α_z equal to 0, 1, 100 and 1000 are shown in Figs. 19 to 22, while Fig. 23 to 26 are for a continuous beams under a uniformly distributed load with α_z equal to 0, 1, 100 and 1000. In all cases, the loading is at the top flange level.

Similar results can be observed from this study as in two-span beams. As would be expected, when α_z is equal to zero the buckling mode for three-span continuous beams is lateral-torsional. The lateral-distortional buckling loads and lateral-torsional buckling loads are almost identical. The results also again show that as the dimensionless torsional parameter increases, the significance of web distortion is increased. At a value of α_z equal to 100 the buckling mode of the longer span continuous beams is lateral-torsional and as the dimensionless length decreases the buckling mode becomes lateral-distortional. At a value of $\alpha_z = 1000$, the reduction of the lateral-torsional buckling load due to web distortion is significant. The results for the compact I-section 200UC46.2 show that the lateral-torsional buckling loads are not affected by web distortion, and the buckling solutions for lateral-torsional and lateral-distortional buckling are almost identical.

At a lower value of torsional stiffness ($\alpha_z = 0$ and 1), the 'design by buckling analysis' in AS4100 (1998) is generally conservative except for short span of continuous beams subjected to a central concentrated load but as the torsional stiffness is increased the prediction of 'design by buckling analysis' in AS4100 (1998) is unconservative. The results of beam under a uniformly distributed loads show that the prediction of the 'design by buckling analysis' in AS4100 (1998) is generally unconservative. As α_z is increased disparity between 'design by buckling analysis' in AS4100 (1998) and lateral-torsional buckling load is increased.

4. Conclusions

The inelastic buckling behaviour of continuously restrained two and three-span continuous beam subjected to a concentrated load and a uniformly distributed load applied at the top flange is investigated using the finite element method. The buckling results show that when the continuous beams are fully restrained against translation only, the buckling mode of beam is lateral-torsional with insignificant distortional effects. As the dimensionless torsional restraint stiffness increases the buckling mode beam became lateral-distortional. At a higher value of α_z , the results show that the cross-section displayed significant distortion, which results in a reduction of the lateral-torsional buckling load due to web distortion being significant. Furthermore, the nominal buckling load obtained from 'design by buckling analysis' in AS4100 has been compared with the inelastic buckling results obtained from this study. This study has found that 'design by buckling analysis' in AS4100 (1998) is generally unconservative.

References

- Abdel-Sayed, G. and Aglan, A.A. (1973), "Inelastic lateral torsional buckling of beam columns", *Publications, IABSE*, **33-II**, 1-16.
- Bradford, M.A. and Gao, Z. (1992), "Distortional buckling solutions for continuous composite beams",

- J. Struct. Eng.*, ASCE, **118**(1), 73-89.
- Bradford, M.A. and Johnson, R.P. (1987), "Inelastic buckling of composite bridge girders bear internal supports", *Proc. of Institution of Civil Engineers*, London, **83**, Part 2, 143-159.
- Bradford, M.A. and Trahair, N.S. (1982), "Distortional buckling of thin-web beam-columns", *Eng. Struct.*, **4**, 2-10.
- Bradford, M.A. and Trahair, N.S. (1986), "Inelastic buckling tests on beam-columns", *J. Struct. Eng.*, ASCE, **112**(3), 538-549.
- Broken Hill Proprietary Co. Ltd, (1988), *BHP Hot Rolled Products*, BHP Co. Ltd, Melbourne, Australia.
- Cuk, P.E., Rogers, D.F. and Trahair, N.S. (1986), "Inelastic buckling of continuous steel beam-columns", *J. Constr. Steel Res.*, **6**, 21-52.
- Dawe, J.L. and Kulak, G.L. (1984), "Plate instability of W shapes", *J. Struct. Eng.*, ASCE, **110**(6), 1278-1291.
- Dekker, N.W., Kemp, A.R. and Trincherro, P. (1995), "Factors influencing the strength of continuous composite beams in negative bending", *J. Constr. Steel Res.*, **34**(2-3), 161-185.
- Essa, H.S. and Kennedy, D.J.L. (1994), "Station square revisited: distortional buckling collapse", *Canadian Journal of Civil Engineering*, **21**(3), 377-381.
- Fukumoto, Y. and Galambos, T.V. (1966), "Inelastic lateral-torsional buckling of beam-columns", *J. Struct. Div.*, ASCE, **92**(ST2), 41-61.
- Haaijer, G. (1957), "Plate buckling in the strain-hardening range", *J. Eng. Mech. Div.*, ASCE, **83**(EM2), 1212.1-47.
- Hall, A.S. and Kabaila, A.P. (1986), *Basic Concepts of Structural Analysis*, GreenwichSoft, Sydney.
- Hancock, G.J. and Trahair, N.S. (1979), "Lateral buckling of roof purlins with diaphragm restraint", *Civil Engineering Transactions*, Institution of Engineers, Australia, **CE21**, 10-15.
- Johnson, R.P. and Bradford, M.A. (1983), "Distortional lateral buckling of unstiffened composite bridge girders", *Int. Conf. on Instability and Plastic Collapse of Steel Structures*, Manchester, Granada, 569-580.
- Kemp, A.R., Dekker, N.W. and Trincherro, P. (1995), "Differences in inelastic properties of steel and composite beams", *J. Constr. Steel Res.*, **34**(2-3), 187-206.
- Kitipornchai, S. and Trahair, N.S. (1975), "Inelastic buckling of simply supported steel I-beams", *J. Struct. Div.*, ASCE, **101**(ST7), 1333-1347.
- Lee, D.S. (2004), "Inelastic buckling of simply supported beams subjected to transverse loading method", Submitted for publication.
- Lee, D.S. and Bradford, M.A. (2002), "Inelastic lateral-distortional buckling of continuously restrained rolled I-Beams", *Steel and Composite Structures*, **2**(4), 297-314.
- Lee, D.S. and Bradford, M.A. (2003), "Inelastic distortional buckling of cantilevers", *Steel and Composite Structures*, **3**(1), 1-12.
- Standards Australia. (1998), AS4100-Steel Structures, S.A., Sydney, Australia.
- Timoshenko, S.P. and Woinowsky-Krieger, S. (1959), *Theory of Plates and Shells*, McGraw Hill, New York.
- Trahair, N.S. (1993), *Flexural-Torsional Buckling of Structures*, Chapman and Hall, London.
- Trahair, N.S. and Kitipornchai, S. (1972), "Buckling of inelastic I-beams under uniform moment", *J. Struct. Div.*, ASCE, **98**(ST11), 2551-2566.